

Surveys in Geophysics

ARCHAEOGEOPHYSICAL BASED APPROACH FOR INCA ARCHAEOLOGY: OVERVIEW AND ONE OPERATIONAL APPLICATION

--Manuscript Draft--

Manuscript Number:	GEOP-D-18-00067R3
Full Title:	ARCHAEOGEOPHYSICAL BASED APPROACH FOR INCA ARCHAEOLOGY: OVERVIEW AND ONE OPERATIONAL APPLICATION
Article Type:	S.I. : New perspectives on geophysics for archaeology
Keywords:	Archaeo-geophysics; GPR; Geomagnetometry; Chachabamba; Inca archaeology
Corresponding Author:	Nicola Masini Istituto per i Beni Archeologici e Monumentali Consiglio Nazionale delle Ricerche Tito (PZ), Basilicata ITALY
Corresponding Author Secondary Information:	
Corresponding Author's Institution:	Istituto per i Beni Archeologici e Monumentali Consiglio Nazionale delle Ricerche
Corresponding Author's Secondary Institution:	
First Author:	Nicola Masini
First Author Secondary Information:	
Order of Authors:	Nicola Masini Luigi Capozzoli Gerardo Romano Dominika Sieczkowska Maria Sileo Jose Bastante Fernando Astete Victoria Mariusz Ziolkowski Rosa Lasaponara
Order of Authors Secondary Information:	
Funding Information:	
Abstract:	Even if in the last decades the use of remote sensing technologies (from satellite, aerial and ground) for archaeology is stepping in its golden age, in Southern America, the geophysics for preventive archaeology is more recent and less used compared to Europe, Central America, and Middle East. . In this paper, we provide a brief overview, and show the preliminary results obtained from the investigations conducted in Chachabamba (Peru). The archaeological area is located on a strategic terrace overlooking three Inca roads, which served the most important ceremonial centres (including Machu Picchu) of the Urubamba Valley also known as the Sacred Valley. In particular, Chachabamba investigations were conducted with two principal aims : 1) to give new impetus to archaeological research with targeted investigations aimed at improving and completing the site's knowledge framework; 2) to experiment and validate an archeogeophysical approach to be re-applied in other sites of the Urubamba valley, including Machu Picchu, having similar characteristics as those found in Chachabamba.
Response to Reviewers:	We thank the Guest Editor for the valuable suggestions and corrections which have been addressed contributing to the improvement of the paper

1 ARCHAEOGEOPHYSICAL BASED APPROACH FOR INCA ARCHAEOLOGY: OVERVIEW
2 AND ~~AN-ONE~~ OPERATIONAL APPLICATION

3
4
5 **Nicola Masini^{1*}, Luigi Capozzoli², Gerardo Romano³, Dominika Sieczkowska⁴, Maria Sileo¹,**
6 **Jose Bastante⁵, Fernando Astete Victoria⁶, Mariusz Ziolkowski⁴, Rosa Lasaponara²**

7 1 Institute for Archaeological and Monumental Heritage, National Research Council C.da Santa
8 Loja, 85050, Tito Scalo (PZ), Italy; E-mail: n.masini@ibam.cnr.it (N.M.), m.sileo@ibam.cnr.it
9 (M.S.)

10 2 Institute of Methodologies for Environmental Analysis, National Research Council C.da Santa
11 Loja, 85050, Tito Scalo (PZ), Italy; E-Mail: luigi.capozzoli@imaa.cnr.it (L.C.),
12 rosa.lasaponara@imaa.cnr.it (R.L.)

13 3 University of Bari, Italy; E-mail: gerardo.romano@uniba.it (G.R.)

14 4 University of Warsaw, Centre for Pre-Columbian Studies, Poland, E-mail:
15 dominika.sieczkowska@gmail.com (D.S.); mziolkowski@uw.edu.pl (M.Z.)

16 5 Ministerio de Cultura Cusco -Programa de Investigaciones Arqueologicas e Interdisciplinarias en
17 el Santuario Historico de Machu Picchu, Peru, e-mail: jose.bastante@gmail.com (J.B)

18 6 Ministerio de Cultura Cusco -Santuario Historico de Machu Picchu, Peru; e-mail:
19 fastetemachupicchu@yahoo.es (F.A.)

20 *Corresponding author: n.masini@ibam.cnr.it
21

22 **Abstract.**

23 Even if in the last decades the use of remote sensing technologies (from satellite, aerial and
24 ground) for archaeology is stepping in its golden age, in Southern America, the geophysics for
25 preventive archaeology is more recent and less used compared to Europe, Central America, and
26 Middle East. . In this paper, we provide a brief overview, and show the preliminary results obtained
27 from the investigations conducted in Chachabamba (Peru). The archaeological area is located on a
28 strategic terrace overlooking three Inca roads, which served the most important ceremonial centres
29 (including Machu Picchu) of the Urubamba Valley also known as the Sacred Valley. In particular,
30 Chachabamba investigations were conducted with two principal aims :

31 1) to give new impetus to archaeological research with targeted investigations aimed at
32 improving and completing the site's knowledge framework;

33 2) to experiment and validate an archeogeophysical approach to be re-applied in other sites of
34 the Urubamba valley, including Machu Picchu, having similar characteristics as those found in
35 Chachabamba.
36

37 **Keywords:** Archaeo-geophysics; GPR; Geomagnetometry; Chachabamba; Inca
38 archaeology
39

Field Code Changed

Field Code Changed

40 1. Introduction

41 In the last decades the use of remote sensing technologies (from satellite, aerial and ground) for
42 archaeology are stepping in a golden age characterized by an increasing growth of both classical
43 and emerging multidisciplinary methodologies, addressed to the study, documentation and
44 conservation of cultural property (Kvamme 2003; Lasaponara & Masini 2008; Lasaponara et al.
45 2016; Cuca & Hadjimitsis 2017; Opitz & Hermann 2018; Masini et al. 2018). The digital tools
46 nowadays available for archaeology enable us to get extremely precise results in a non invasive way
47 and to speed up the work during the diverse phases of archaeological investigations ranging from
48 survey, mapping, excavation, and monitoring at diverse scales of interest, moving from small
49 artefacts to architectural structures and landscape reconstruction. This has totally revolutionised the
50 classical approach of studying human past and activities, before mainly based on the recovery and
51 analysis of material culture, field recognition, survey, test pits, and, finally, excavation campaigns.
52 All of these activities are time consuming, expensive, and can produce destructive impacts. Time,
53 costs and invasive impact can be reduced or optimized through archaeological prediction tools and
54 methods, as earth observation technologies including remote sensing and geophysics. The use of
55 these technologies is particularly important in absence of historical sources, as in the case of
56 prehistoric archaeology or for studies of civilizations that did not have writing and did not leave any
57 documentation. This is the case of pre-Hispanic civilizations in Peru and in other countries of
58 Southern America, from the most ancient cultures, as Chavin, Nasca and Moche, to the most recent
59 ones including Inca. Despite this and the fact that the first pioneering geophysical application in
60 Southern America date to 1985 (Gumaer1985), the geophysics for the study of the Andean
61 civilizations is still today generally not used in the operational activities of preventive archaeology.

62 However, it must be considered that even in Europe and North America, the use of geophysics in
63 archaeology has strongly increased only in the last two decades thanks to the technological
64 advances of instrumentation, availability of friendly data processing tools, improvements in data
65 visualization which facilitate the interpretation of the results.

66 In Southern America, the use of geophysics for archaeological prospection started at the end of
67 the first decade of the 2000s. The most popular geophysical techniques used for preventive
68 archaeological research, are geomagnetometry, Ground Penetrating Radar (GPR) and Electrical
69 Resistivity Tomography (ERT), selected according to the expected characteristics of both buried
70 archaeological features and soils.

71 Geomagnetometry methods, based on the measuring and recording of spatial variations in the
72 Earth's magnetic field, have been mainly used to detect and map (i) ring ditches of the prehistoric
73 sites in the lowlands of the Llanos de Moxos in the Bolivian Amazonia (Prümers 2006) and (ii)
74 buried earthen city walls of the ceremonial center of Pachacamac in Peru (Lasaponara et al. 2017).

75 GPR, based on the analysis of radar signal reflection in the presence of subsoil discontinuities,
76 has been mainly exploited to detect: (i) stone masonry structures, as those in andesite identified in
77 Tiwanaku (Henderson 2004), and (ii) naturally dried-earth settlements, from the Formative age in the
78 northwest of Argentina to the colonial period in Patagonia (Bonomo et al. 2010; Lascano et al.

79 2003). GPR has been also fruitfully employed in Peru for the characterization of looted areas in
80 Ventarron (Lasaponara et al. 2014).

81 Integrated geophysical methods, including ERT, are adopted where and when the use of a single
82 geophysical method is not suitable and effective in terms of information quality, data resolution and
83 penetration capability. For sake of brevity, we cite the discovery in 2012 of a Nasca pyramid in the
84 ceremonial center of Cahuachi made by integrating GPR and ERT (Masini et al. 2016). The joint
85 use of GPR and Magnetic methods proved to be complementary in detecting several different
86 archaeological features from (i) the buried foundation trenches of quincha (a construction system
87 using wood and cane) walls of the colonial villages in the Zaña Valley (North Peru)
88 (Vanvalkenburgh et al. 2015), to (ii) the Nasca tombs and ritual offerings in Cahuachi (Rizzo et al.
89 2010).

90 Related to Peru, it must be considered that paradoxically geophysical investigations were mostly
91 performed along the arid coast areas to detect raw earth material settlements, which still today
92 represents a technical challenge due to the very low geophysical difference/contrast between the
93 targets and the neighbouring areas. On the contrary, in the highland of Peru very few archaeo-
94 geophysical investigations have been performed to investigate settlements in stone, easier to be
95 detected compared to those in earth material. In particular in the Urubamba valley, the origin region
96 of the Incas, which includes Machu Picchu (the most famous and visited pre-Hispanic sites of Peru
97 geophysical prospections were only performed for the monitoring of the landslide hazard to map
98 fractures and zones of weakness in crystalline bedrock (Best et al. 2009).

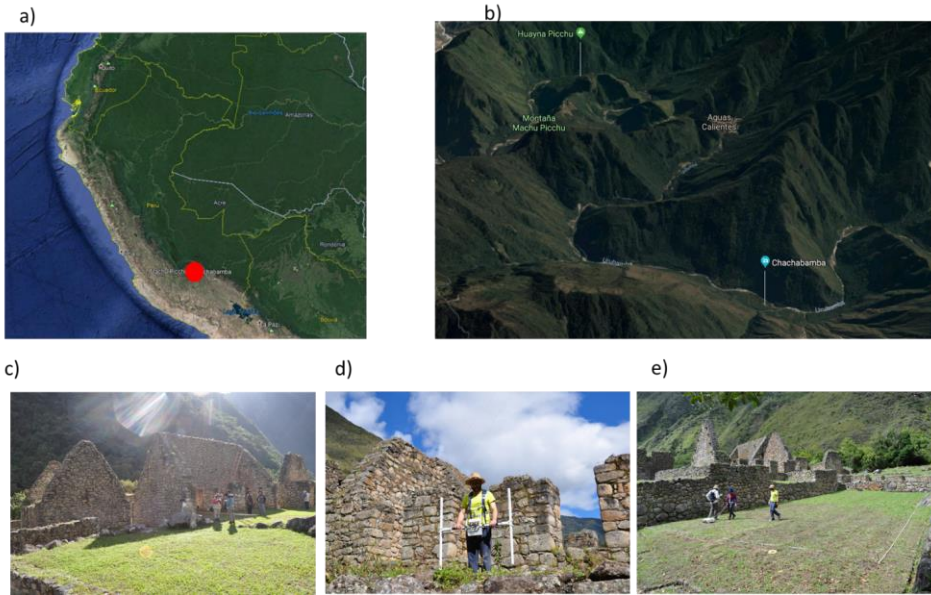
99 In Machu Picchu as also in the Urubamba valley, up to now no significant archaeological studies
100 have been performed using geophysical methods or other earth observations techniques. To fill this
101 gap, a specific archaeological project in Urubamba valley started in 2017 as bilateral cooperation
102 between the ITACA Mission of Italian CNR and the University of Warsaw in the framework of an
103 agreement with Ministerio de Cultura del Peru. The aim of these joint research activities is to
104 explore new approaches and investigation tools using the most advanced earth observation sciences
105 and technologies to advance our knowledge on the Inca civilization, to improve our understanding
106 of the Inca sites and their relationship with environment.

107 In this paper, we discuss the preliminary results obtained from the investigations conducted in
108 Chachabamba. It is located on a strategic terrace overlooking three Inca roads, which served the
109 most important ceremonial centres (including Machu Picchu) of the Urubamba Valley also known
110 as the Sacred Valley. In particular, Chachabamba investigations were conducted with two principal
111 aims :

112 1) to give new impetus to archaeological research with targeted investigations aimed at
113 improving and completing the site's knowledge framework;

114 2) to experiment and validate an archeogeophysical approach to be reapplied in other sites of the
115 Urubamba valley, including Machu Picchu, having similar characteristics as those typically found
116 in Chachabamba, i.e. typical Inca walls, with their constructive features, terracing systems, and
117 water channeling.

118



119
120

121 Figure 1. a: Peru with location of Chachabamba in Peru; b: location of Chachabamba in Urubamba valley
 122 where important Inca ceremonial and administrative centers, including Machu Picchu, overlook; c-d-e:
 123 geophysical data acquisition including geomagnetic (d) and georadar (e).

124
125

126 **2 Study area**

127 *2.1 Geographical context*

128 The Chachabamba archaeological site is part of the Historic Sanctuary of Machu Picchu and is
 129 located over an alluvial terrace at an altitude of 2170 m , on the left side of the Vilcanota River and
 130 the right bank of the Chachabamba basin. Three Inca roads connect the site to the most important
 131 ceremonial and administrative centers in the area, such as Wiñaywayna, Condorpata, Choquesuysuy,
 132 Chaskapata, Killapata and Machu Picchu. Chachabamba covers approximately 19,000 m² and
 133 develops in a reduced slope area that is located along the bottom of the Urubamba river valley, an
 134 alluvial surface of Quaternary origin.

135

136 *2.2 Geological and geomorphological setting*

137 From the geological point of view, ~~it~~the site is characterized by the outcrop of granitic intrusive
 138 materials that are part of the eastern Cordillera of southern Peru. In particular, intrusive

139 permotriassic rocks and intrusive igneous rocks, part of the so-called Machul Pictu Batolite, are
140 essentially consisting of granites and granodiorites (Carlotto et al 2009) which develop for a very
141 large area of the Chachabamba site, including the slopes to the north and south.

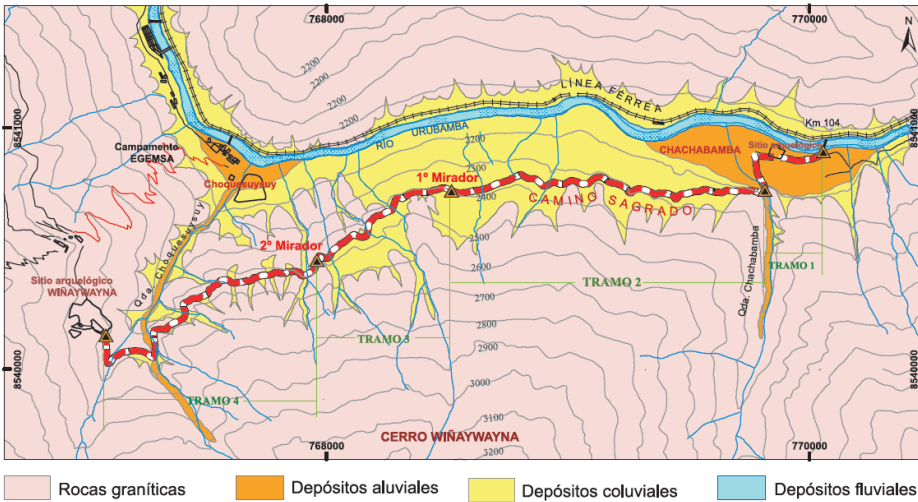
142 The batholitic complex of Permian / Triassic age in the Eastern Cordillera (between the High
143 Plateau and Subandine Zones of the Peruvian Andes- consists essentially of white to gray-colored
144 granite which are characterized by abundance of quartz, feldspar and mica, predominantly biotite.
145 There are also local rocks as granodiorites and serpentinites.

146 The Urubamba River crosses the eastern Cordillera of southern Peru (Fig. 2), locally called
147 Cordillera Vilcabamba, and forms the canyon of Urubamba. The south-west and north-eastern
148 slopes of the valley are rather steep and have important mountain peaks including the Salcantay
149 (6,264 m asl) and Huamantay (5,459 m asl) to the southwest of Nevada Veronica (5,750 m asl) and
150 Bonanta (5,024 ~~mmmmmm~~ m asl) to the northeast (Carlotto et al 2009). At the foot of the snow-covered
151 glaciers, U-shaped valleys, moraines and other of recent and ancient glaciations are present, while
152 along the Urubamba river there are widespread deposits of the eluvial, colluvial and alluvial
153 deposits dated back to the Quaternary.

154 The archaeological site of Chacabamba is built right on alluvial deposits formed by accumulation
155 resulting from the dismantling of the Machu Picchu batholith. In particular, it is settled in an area
156 where the tributary Chachabamba flows and has a large recharge area inside the Urubamba. In fact,
157 in this area essentially quaternary deposits of disassembly of the batholith emerge. The latter, in its
158 last section starting from Chachabamba, is imposed on colluvial deposits and sometimes on granites
159 or alluvial soils as showed in the geological map from Carlotto et al 2011.

160 The colluvial deposits have several meters of thickness and are located on the slopes of the
161 Wiñaywayna hill and form a surface mantle characterized by the mixture of rock fragments of
162 gravel granulometry up to the size of the blocks. Alluvial deposits are recognized at the mouths of
163 the Chachabamba and Choquesuysuy rivers, with greater development at Chachabamba and are
164 formed by large blocks of granite in a clayey and sandy clayey matrix. These deposits are very
165 unstable, especially in the presence of heavy rains as they immediately reach saturation status.

166



167
 168 Fig 2 – Geologic map of Chahabamba site (from Oviedo et al 2011)
 169

170 *2.3 Archaeological context and state-of-the art of investigations*

171 Chachabamba was investigated for the first time in 1941 by Wenner Gren who unearthed terraces,
 172 baths and water channels supplying the baths (Fejos 1944). These findings suggested that
 173 Chachabamba was an important religious place for the worshipping of water and fertility goddesses.
 174 The Inca had a functional and mystic connection with the nature. They were able to develop
 175 innovative agricultural techniques for plant adaptation taking into account climate and microclimate
 176 conditions, as in the case of the Moray site (Plachetka 2015), and the Mother Earth (Pachamama)
 177 and water were founding elements in the Incas cult and worldview.

178 After the excavations that took place in 1941, other investigations were carried out in 1996-97 only
 179 with the purpose of the restoration of the site conducted by the Instituto Nacional de Cultura.
 180 Finally, in 2016, first scientific excavations were conducted in the framework of the "Programa de
 181 Investigaciones Arqueológicas e Interdisciplinarias en el Santuario Histórico de Machupicchu and
 182 Centro de Estudios Andinos de la Universidad de Varsovia en el Cusco". These investigations
 183 provided invaluable information on the use and function of the architectural spaces. In particular,
 184 the investigated area (see figure 2) is the typical *kancha*, that develops around a central open space
 185 (with buildings facing inside) enclosed by walls to form small courtyards in the junction areas
 186 (Gavazzi 2010). In Chachabamba the *kancha* is structured around two squares (plaza 1 and plaza 2)
 187 flanked by buildings, known as *wayranas*, laid out symmetrically along north-south and east-west
 188 axes. The two squares are divided by a central building. The *wayranas* are built with a masonry

189 consisting of carefully laid field granite stones with finished corners and adobe binders and
190 characterized, in some cases (at south of the central building), by niches (Fejos 1944). They are
191 composed of two or more rectangular rooms which served to host pilgrims. In fact, Chachabamba
192 was also a checkpoint for people on route to other sanctuaries, among which *in primis*, the
193 sanctuary of Machu Picchu.

194 A 'boulder shrine' (named *huaca* in quechua) borders the north side of plaza 1 and overlooks the
195 river below. It is a partially worked granite outcrop serving as an altar, smoothed off on the top,
196 with two seats cut into it as well as a little flight of four stairs at one side of the seats (Fejos 1944)
197 .Regarding the construction materials, the survey showed that in the vast majority of cases the walls
198 were made in granite, extracted on site.

199 The architectural complex of *plazas* and *wayranas* is flanked to the east and west side by two broad
200 terraces, which were '*plazas undidas*' (sunken squares) characterized by the presence of ceremonial
201 baths on the north and south side (see map in Figure 2).

202 Chachabamba presents all the typical architectural and functional features which could be found in
203 the ceremonial and administrative sites of Urubamba valley, as the two plazas which recall the
204 'sacred-plaza' at Machu Picchu, the boulder shrine and the baths with ceremonial significance which
205 are similar to those in one of the plaza of Phuyu Pata Marka (Fejos 1944).

206

207 **3. Material and methods**

208 The archaeogeophysical investigations have been focused on some areas of Chachabamba
209 archaeological site (figure 3), including the *plazas hundidas*, the central square, the surroundings of
210 the ceremonial baths and the altar. The aim is to provide an archaeological prediction map to guide
211 future excavations and investigations and to detect the presence of past constructive phases hidden
212 or reworked, related to masonry structures, canals, ceremonial baths. Finally, another expected
213 result is the setup and validation of a geophysics-based investigation approach to be used in other
214 sites of Urubamba valley which will be soon investigated by the Italian-Polish mission. To the aim
215 of our purposes, magnetometry and ground penetrating radar were used: i) the first one was adopted
216 to detect ditches, shallow canals and walls, ii) the second one to identify deeper walls (up to 2m
217 depth), canals, buried earthworks and terraces.

218 The results from magnetometric and GPR investigations have been jointly analyzed and interpreted
219 in a comparative way in order to maximize the information content exploiting their
220 complementarities in detecting features of archeological interest.

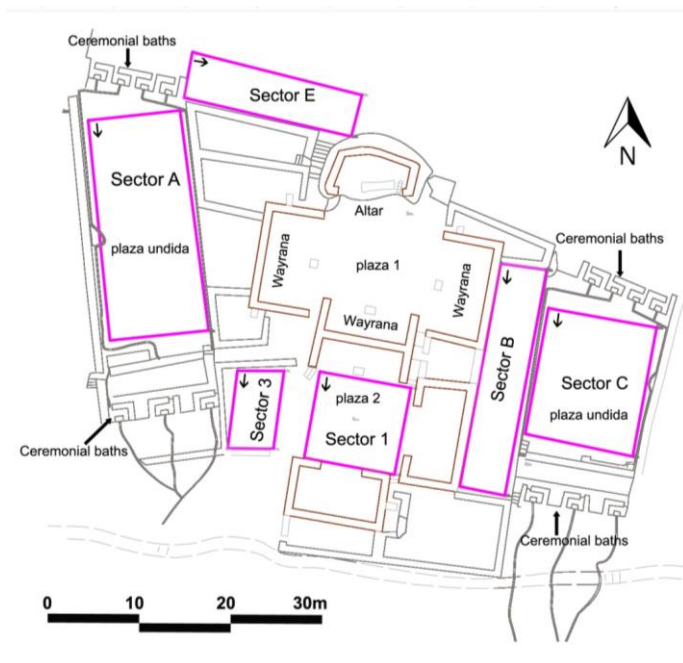
221

222

Formatted: Font: Italic

Formatted: Font: Italic

Formatted: Font: Italic



223
 224 Figure 3. Chachabamba: investigated areas. The arrows in the corners of the investigated areas
 225 indicate the starting point and the direction of the geophysical data-acquisition. The map includes
 226 the most important functions of the sacred areas.

227

228 *3.1 Geophysical methods used for the study area*

229 *3.1.1 Ground penetrating radar (GPR)*

230 GPR is a non-invasive methodology used in geophysics to detect and characterize
 231 electromagnetic (e.m.) impedance contrasts in a medium. It is based on the analysis of the
 232 reflections of electromagnetic waves transmitted into the ground. This method provides information
 233 on subsoil from a depth of some meters up to a few tens of meters according to the frequency of the
 234 electromagnetic waves and the electrical characteristics of the potential targets and surrounding soil
 235 (permittivity and electrical conductivity). The use of different antennas and frequencies enables the
 236 imaging of subsoil at different penetration depths and with different details. Lower the frequency
 237 greater the penetration, for this the operating frequency is always a trade-off between resolution and
 238 penetration. Moreover, the use of different antennas and frequencies enables multiple imaging at
 239 different resolutions and penetration capabilities and for different purposes and application fields
 240 ranging from civil and geotechnical engineering; geological and sedimentological studies,
 241 environmental contamination, monitoring of monuments and artifacts, and archaeological research.

242 The use of GPR in archeology dated back to the 1970s, and more recently (from 1990) it has
243 been quite systematically adopted to detect and map subsurface archaeological artifacts, features,
244 and patterning, changes in material properties, and voids. Indeed, its success in the archaeological
245 prospection field is showed by the great number of researches where the method is used in order to
246 detect buried structures in urban and rural areas and discover archaeological features in a great
247 number of scenarios, such as to identify ancient settlements (Trinks 2014), locate unearthed burials
248 and ceremonial offering (Leucci et al. 2016; Pipan et al. 2001) reconstruct the history of ancient
249 buildings (Goodmann and Piro 2008; Masini et al. 2017), image structures and infrastructure
250 (Malfitana et al. 2015; Florit et al. 2018), identify sub-water structures (Qin et al. 2018; Ludeno et
251 al. 2018).

252 From the technical point of view, GPR device is made up of (i) an antenna (operating in both
253 transmitting and receiving mode), (ii) a control unit, (iii) battery supply and (iv) a survey cart. The
254 antenna (operating in transmitting mode) propagates e.m. wave in the subsoil and receives
255 (operating in receiving mode) the e.m. wave back reflected by discontinuities i.e. depositional
256 layers and/or buried "objects" in order to define a mono-dimensional description of e.m. impedance
257 contrasts encountered by the generated signal called A-Scan. The emitted signal is repeated,
258 according to a defined cadence and the GPR is moved progressively along a predetermined path on
259 the surface, so that a two-dimensional representation is obtained ("B-scan or Radargram"). To
260 calculate the depth of the reflections, it is necessary to determine the propagation speed of the radar
261 waves in the investigated levels. This is mainly related to the physical-electrical characteristics of
262 the investigated medium (in particular it is inversely proportional to the square root of the dielectric
263 constant ϵ) and is estimated or calculated through various possibilities of signal analysis or with
264 experimental calibration tests. The data processing enables us to convert the propagation speed of
265 the radar waves into the subsoil depth. Finally, the digital acquisition allows us to represent the
266 acquired data in 2d-profiles that can be filtered and enhanced to detect and locate archaeological
267 features or changes in the matrix referable to different historical phases of the site.

268 For the detailed characterization of the target it is necessary to analyze the lines of GPR data
269 which represent a sectional (profile) view of the subsurface usually acquired at 0.50 to 1.0m
270 distance between each other (defined according to the size of the expected target).

271 The use of multiple lines of data, systematically collected over the investigated area, is generally
272 used to obtain three-dimensional representations of the scattering phenomena occurring within the
273 subsoil. Data can be visualized as three-dimensional blocks, or as horizontal or vertical slices. In
274 particular, horizontal slices generally indicated as "depth slices" or "time slices", are maps related to
275 specific depths. In archaeological applications, time-slicing is usually adopted because the presence
276 of horizontal patterning is an important indicator of anthropogenic/cultural activities. Nevertheless,
277 even if horizontal sections are the most common and easy way to visualize the pattern of targets,
278 especially for large areas, sometimes, this visualization can compromise the reliability of the
279 information, especially for morphologically irregular surfaces and complex structures located at
280 different depths (Masini et al. 2017).

281
282

283

3.1.2 Magnetic method

284 In non-destructive archaeological explorations the magnetic survey is one of the most important and
285 widely applied geophysical techniques (Larson et al. 2003). The aim of a magnetic survey is to
286 investigate the subsurface on the basis of the anomalies in Earth's magnetic field resulting from the
287 magnetic properties of the underlying rocks or buried artifacts.

288 The origin of Magnetic anomalies within the Earth's magnetic field can be related either to the
289 induced or the remanent magnetism. With the term induced magnetism it is indicated the properties
290 according to which an unmagnetized magnetic material within the earth's magnetic field becomes
291 magnetized. The induced magnetization is directly proportional to the intensity of the ambient field
292 and to the magnetic susceptibility of the magnetized material. The remanent magnetism, on the
293 contrary, is the magnetism that an object has also in absence of a magnetic field. The remanent
294 magnetism is the results of several processes (i.e. thermal or chemical) and it may differ radically
295 from induced field (always the same direction of the inducing field).

296 In archaeological explorations, both the induced and the remanent magnetization are very important
297 (Aspinall et al. 2008). The former is useful to highlight the variations in magnetic susceptibility
298 between topsoil, subsoil and rocks; induced magnetization allows hence to detect the possible
299 presence of ditches, pits and other silted-up features which were excavated in ancient times and then
300 silted or backfilled with topsoil. The remanent magnetization, on the other hand, makes possible to
301 sense the presence of man-made objects which were heated (pottery kiln, hearth), of volcanic or
302 metamorphic stones or of bricks.

303 The range of magnetic anomalies (related both to the induced and the remanent magnetization)
304 generated by buried archaeological features spans from few nT (1–20 nT) for remains up to
305 thousands of nT for fired' structures (hearths, kilns, crockery, pottery) and ferrous objects (Piro et
306 al. 2007).

307 For the aforementioned reasons, and being that the magnetic method is characterized by a (i)
308 considerable cost-effectiveness and (ii) extreme speed in the use compared to other survey methods
309 (as GPR and ERT), it has been widely applied in archeology, from the small-scale site
310 characterization (Aitken al. 1958) to the surveying of large scale areas (i.e. Keay et al. 2014).

311

312

313

3.2 Geophysical data acquisition and processing

314

3.2.1 GPR data acquisition and processing

315 GPR surveys were performed with a RIS MF Hi-Mod GPR System of IDS equipped with an
316 array of two multi-frequency antennas using simultaneously 200 and 600 MHz antennas mounted
317 on a survey cart equipped with an incremental encoder. The 200 MHz and 600 MHz data were
318 acquired in continuous and reflection mode with a time window of 130 ns and 160 ns respectively,
319 samples per scan set at 512 with a resolution of 16 bits and a transmit rate of 100 KHz.

320 The data processing is based on several steps addressed to (i) improve the signal noise ratio and
321 (ii) enhance the discontinuities to make the interpretation easier. The data were processed using
322 standard two-dimensional processing techniques by means of the Reflex-W software [Sandmeier,
323 2016].

324 Accurate three-dimensional representations were obtained at different frequencies in order to
325 image potential archaeological targets. The adopted data processing can be summarized as follows:

Formatted: Indent: First line: 2 ch

- 326 1) Normalization of the amplitude (performed on the mean amplitude value of the complete
327 profile) in order to de-clip saturated traces using a polynomial interpolation procedure;
- 328 2) Dewow filter to leave out potential low frequency part of the signal;
- 329 3) Removal of background made (i) summing all the amplitudes of reflections (recorded at the
330 same time along a profile) and (ii) dividing by the number of traces summed. In this way the
331 average of all background noise is subtracted from the data;
- 332 4) Energy decay based on a mean amplitude decay curve determined from all existing traces;
- 333 5) Declipping step to reduce too high amplitudes values;
- 334 6) Bandpass filter to reduce the noise affecting the radargram linked to the gain function
335 previously adopted;
- 336 7) Kirchhoff 2D-velocity migration with a velocity estimated quantitatively using the
337 diffraction hyperbolas generated by potential archaeological features. The adopted velocity is
338 equal to 0.060-0.065 $\text{m}\cdot\text{s}^{-1}$ that is coherent with a scenario characterized by a high water
339 content.

340 After these steps, a 3D representation was built interpolating data of the processed 2D-lines. A
341 linear interpolation was made analyzing an area equal to two times the minimum distance between
342 the radargrams. Then the envelope of each trace of the 3D-file was calculated and showed in
343 horizontal depth slices where the reflections with greater amplitude are highlighted with the aim to
344 support the identification of archaeological features.

345 3.2.2 Magnetic data acquisition and processing

347 The magnetometer used for the investigations carried out at Chachabamba is the Grad601-
348 Bartington. It is a high-resolution fluxgate gradiometer, used to measure minimal variations in the
349 magnetic field that are caused by anomalies hidden in the soil, as archaeological features, tubes,
350 cables or unexploded ordnance. The system includes a data logger, a battery, two Grad-01-1000I
351 sensors mounted on a rigid carrier bar. The instrumental sensitivity is ± 1 nT (nano Tesla).
352 Calibration is performed on-site prior to acquisition through an automated procedure which allows
353 to correct possible misalignment in the sensors measurements.

354 The magnetic gradiometry acquisition technique, compared to the single-sensor measurements, has
355 a reduced depth resolution linked to the fact that gradient field decays with the fourth power of the
356 distance but it allows a simplification of the measuring and analysis of the magnetic data by making
357 them not dependent from magnetic field temporal variations, from the regional background field
358 and from cultural noise.

359 The surveyed area location (13°09'47"S 72°32'44"W) imposes some considerations on the expected
360 results of the magnetic surveys. Since near the equator, the Earth's field is almost horizontal, the
361 way in which the magnetic anomalies can be detected varies according to their orientation. In
362 particular, for a survey performed closer to the equator, the anomalies from north-south oriented
363 object can decrease until they become invisible (Radhakrishna Murthy 1998), therefore, features
364 that extend in a north-south direction may not be detected. Thus considering, the integration with
365 GPR data will be far more important for the detection of N-S elongated features.

366 In the present paper, the magnetic data have been collected in unidirectional mode (considering the
367 relative small extension of the surveyed area, zig-zag mode was not adopted to increase data
368 quality), along parallel profiles 1 m apart. With a walking speed of about 1ms⁻¹, the spatial
369 resolution was about 1 m× 0.1 m.

370 i) The data processing was based on the filtering of the rough magnetic data to obtain the best S/N ratio
371 using the following steps: despiking made using a uniform weighted window to search for and
372 leave out outlier valued replace by the mean;

373 ~~ii) despike to remove the striping effect between grids caused by directional effects;~~

374 ~~iii) pass-band filter, to remove high or low frequency components;~~

375 ~~iii) despike to remove the striping effect between grids caused by directional effects;~~

376 iv) Kringing interpolator with a linear variogram to highlight the main geomagnetic linear
377 anomalies.
378
379

4. Archaeogeophysical investigations: results and discussion

380 The following paragraphs show and discuss some of the results obtained from the GPR and
381 Magnetic prospection (MAG in what follow). It has to be considered that: (i) the GPR slices
382 provide information at different depths, whereas (ii) the gradiometric data only give indication of
383 the maximum possible depth of the source of magnetic anomalies. Therefore, any magnetic
384 anomaly may have a counterpart in all, none or in some of the GPR time-slices. Figure 2 shows the
385 investigated areas. In particular, the archaeogeophysical areas have been indicated with A, B, C, D,
386 E, F, 1 and 3. For sake of brevity only the results on five sectors will be described and discussed.

387 4.1 Sector A: the west *plaza undida* 388

389 The MAG survey was carried out according to pre-established grids and profile spacing of 1 meter.
390 The measures involved an area of size 24x10m following an acquisition direction of N-S. In the
391 same area, the GPR surveys were carried out according to the two directions E-W and N-S with a
392 spacing between the profiles of 0.5 m. GPR investigations were conducted using marker placed
393 every meter.

Formatted: Font: Italic

394 MAG map is shown in fig. 3a. The range of magnetic anomalies, relatively small (10 nT), and on
395 the absence of regular or elongated patterns, make difficult the identification of buried
396 archaeological features 'sic et simpliciter'. The most relevant anomaly located on the west side (a1)
397 of the magnetic map is due to the presence of a rock formation emerging from the field and also
398 mapped in figure 2. Thus, anomaly a1 was generated by a reduction of the distance between the
399 magnetic sensors and the investigated surface; this reduction occurred during the MAG data
400 acquisition when the magnetic sensor passed over this elevated rock formation. Other magnetic
401 anomalies observable on the west side of the magnetic map can be ascribed to the presence of
402 archeological remains such as walls and the channel flanking the west side of the *plaza undida*,
403 which feed the ceremonial baths (see figure 3).

Formatted: Font: Italic

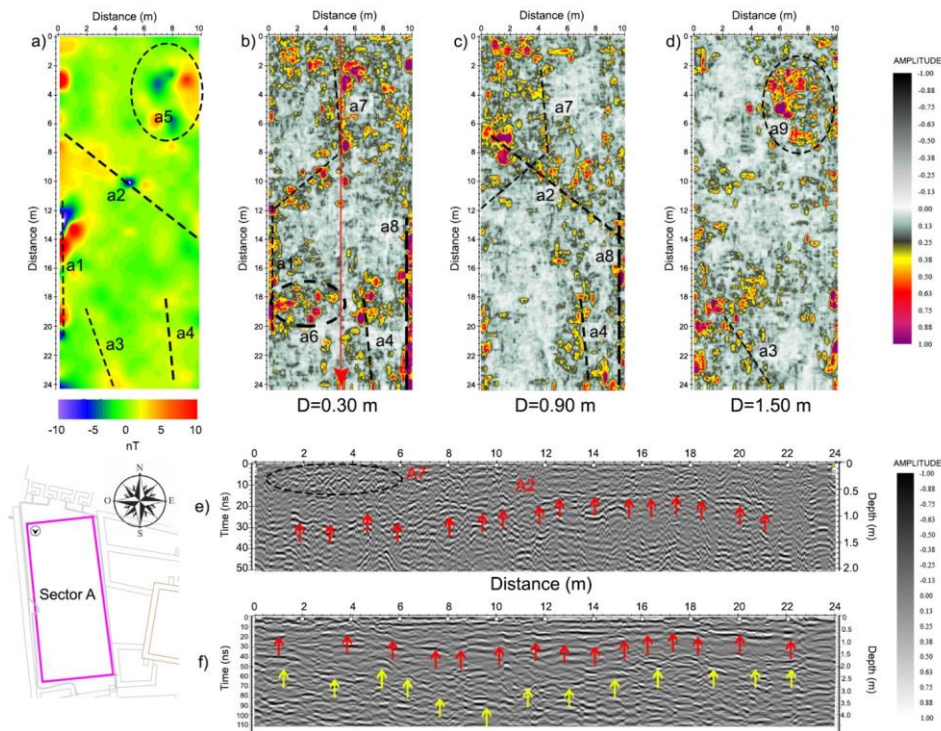
404 Anomalies a3 and a4 seem to converge in a common point and could be associated to the presence
405 of drainage channel. It is worth to note the presence of linear anomalies, indicated with a2, that
406 transversely cross the area, and other anomalies indicated with a5 in the north east corner of *the*
407 *plaza undida*.

Formatted: Font: Italic

408 At first sight, results obtained with GPR are very hard to interpret because of the presence of
409 reflections distributed without break in continuity. To simplify the identification of significant
410 structures from an archaeological point of view some depth slices are extracted by the 3D model
411 generated using the radargrams. The slices highlight the presence of some interesting alignments
412 and reflective areas imputable to archaeological or geological features that confirm geomagnetic
413 results and identify other relevant anomalies. In particular, at a depth of 0.30 m (Fig.4b) some
414 shallow linear structures are detected (a1 and a8) that correspond presumable to some drainage
415 channels. At this depth some reflective areas, a6 and a7, are detected and oriented as the nearest
416 walls and could be associated to archaeological features. A7 anomaly is also detectable at a depth of
417 0.90 m. Anomaly a2, already detected by magnetometric acquisition, is confirmed by the GPR
418 acquisition that identifies it at 90cm depth. Magnetic anomalies a3 and a4 well fit with GPR
419 reflectors at depths of 0.90 and 1.50 meters, respectively.

420 Finally, chaotic and not regular reflections are due to outcropping rocks, as confirmed by trial
421 excavations conducted by archaeologists coauthors of this paper (Ziolkowski 2016; 2017), referred a
422 huanca. For the Inca builder of Chachabamba, the huanca was a sacred monolithic rock with the
423 function as altar (for additional detail about the huanca see Nair 2015, in particular p. 42) . Similar
424 examples of huanca have been found in other Inca ceremonial centers, among which Macchi Picchu
425 where in recent excavations conducted in 2016 a huanca has been found in a plaza hundida
426 (Ziolkowski 2016).

427 Figure 4e-f shows B-scans, acquired at the frequency of 600 and 200 MHz, respectively. They
 428 image the presence of two main stratigraphic units highlighted with red and yellow arrows at
 429 different depths that likely correspond to different archaeological phases of the site. It is remarkable
 430 the strong pseudo-horizontal reflectors that across the whole radargrams, at depths approximately
 431 ranging between 0.50 and 1.00 m (visible both at 600 both 200 MHz), and 2.0 and 3.0 m (detectable
 432 only within data at 200 MHz). It is possible that the first one (see red arrows in figures 4e and 4f) is
 433 related to the presence of anthropic soil while the second one (see yellow arrows in figure 4f)
 434 identifies the expected bedrock.



435
 436
 437 Figure 4. Sector A. (a) Z gradiometric map; (b-c-d) GPR depth slices (600 MHz frequency) at theoretical
 438 depths of 30, 90 cm and 150 cm respectively (red and purple colours indicate reflections with higher
 439 amplitude); (e-f) radargrams acquired at 600 and 200 MHz frequencies respectively in correspondence of the
 440 profile indicated with the red arrow in figure 3b. Red and yellow arrows mark the presence of two main
 441 stratigraphic units likely corresponding to different archaeological phases of the site

442
 443 **4.2 Sector B**

444 MAG survey was carried out according to a grid of 24x5 meters (Fig. 5a) following a north-south
445 acquisition direction and with a distance between measurements of one meter. In the same area,
446 GPR surveys only in the longitudinal direction were carried out from north to south and with a
447 spacing between the profiles of 0.5 m.

448 MAG results, as showed in figure 4a, have identified the possible presence of an anomaly b1
449 perpendicular aligned with an existing wall located at west of the map; further some disorganized
450 anomalies are recorded near the south edge of the area (b5) that could be associated to removed
451 material or collapsed structures. In this zone also a linear anomaly (b4) characterized by an
452 orientation not compatible with that of existing structures was also recorded.

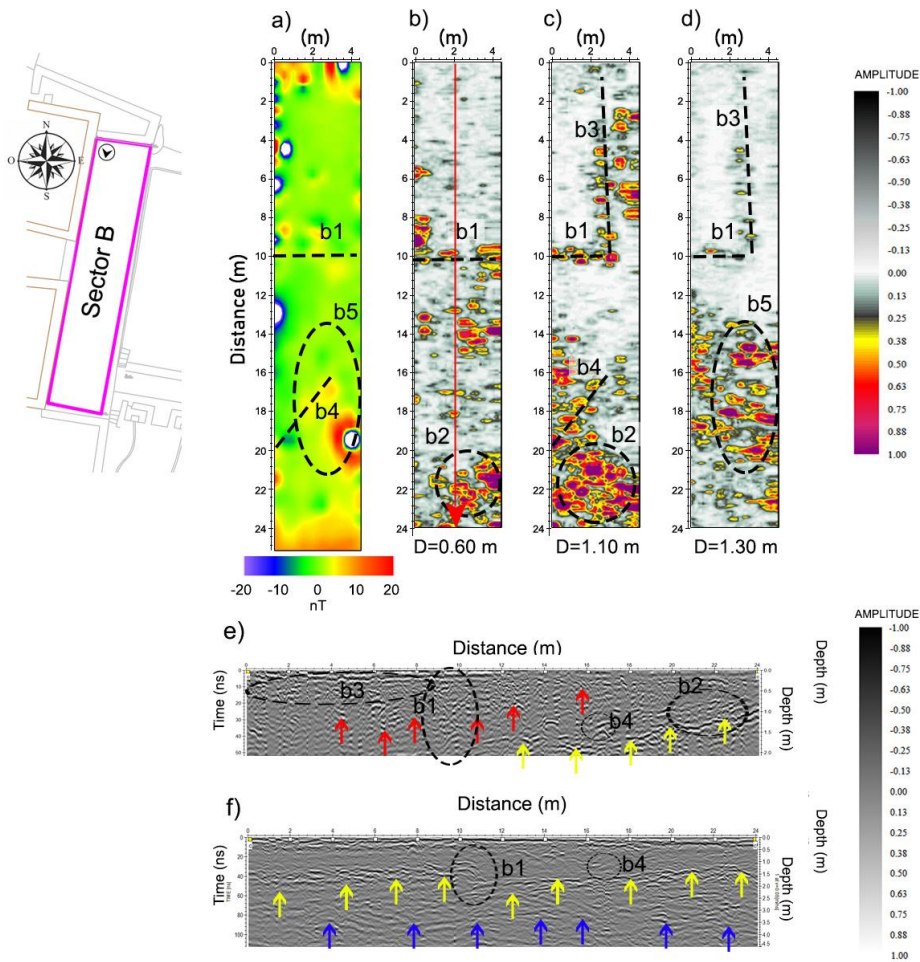
453 GPR results have identified the presence of some aligned reflections (b1) in continuity with the near
454 walls that confirm the MAG results. Further a perpendicular structure, indicated with b3, is also
455 recorded at the depths of 0.90 and 1.30 m (see figure 5c and d).

456 The presence of not homogeneous material or collapsed structures could justify the reflective areas,
457 indicated with b2 and b5 in the southern part of the map. Furthermore, GPR map at 1.10m depth
458 puts in evidence a linearly oriented reflective area consistent with magnetic anomaly b4.

459 GPR B-scan show three sub-horizontal layers (see figure 5e and 5f) of archaeological interest. In
460 particular, it is possible to note the presence of a continuous sub-horizontal reflector at a depth
461 ranging between 0.50 and 1 m. It is due to a recent earthmoving works (red arrows) which probably
462 cover the cause of strong reflector visible at a depth of about 1.5 meter and better detectable in the
463 b-scan acquired at the frequency of 200 MHz (see fig. 5f).

464 Finally, at a depth greater than 3 m another reflective layer was recorded that could correspond to
465 the geological soil. The presence of this behaviour leads to hypothesize the presence of some
466 terraces enclosed by walls that are the continuation of the closer ones. This hypothesis is also
467 confirmed by the presence of the reflective alignments b1 and b2 detectable in the depth slices of
468 figure 5b-c-d.

469



470
 471 Figure 5. Sector B: (a) Z gradiometric map; (b-c-d), Depth slices (200 MHz frequency) at depth of about 60
 472 cm, 110 cm, and 130 cm respectively; (e) b-scan acquired at 600 MHz frequency in correspondence of the
 473 profile indicated with the red arrow in Fig.5b; f) b-scan acquired at 200 MHz frequency along the same
 474 profile. Red arrows indicate the position of sub-horizontal reflector due to a recent earthmoving works.
 475 Yellow and blue arrows mark the presence of reflective layers of anthropogenic layers, as confirmed by trial
 476 excavations made close to this area (Ziolkowski 2017)

477
 478

479 **4.3 Sector C**

480 Magnetometric measurements were be made according a grid with a size of 12x14m and
481 acquisitions longitudinal with a distance of 1 meter. GPR surveys were acquired with the same
482 scheme adopted for the magnetometric techniques but in this case the distance between the
483 investigated lines was halved to obtain a better resolution. The presence of furrows for soil
484 irrigation have strongly complicated the acquisition because the investigated surface was not flat
485 and regular and this is the reasons that the surveys were carried out only in parallel to the channel
486 direction.

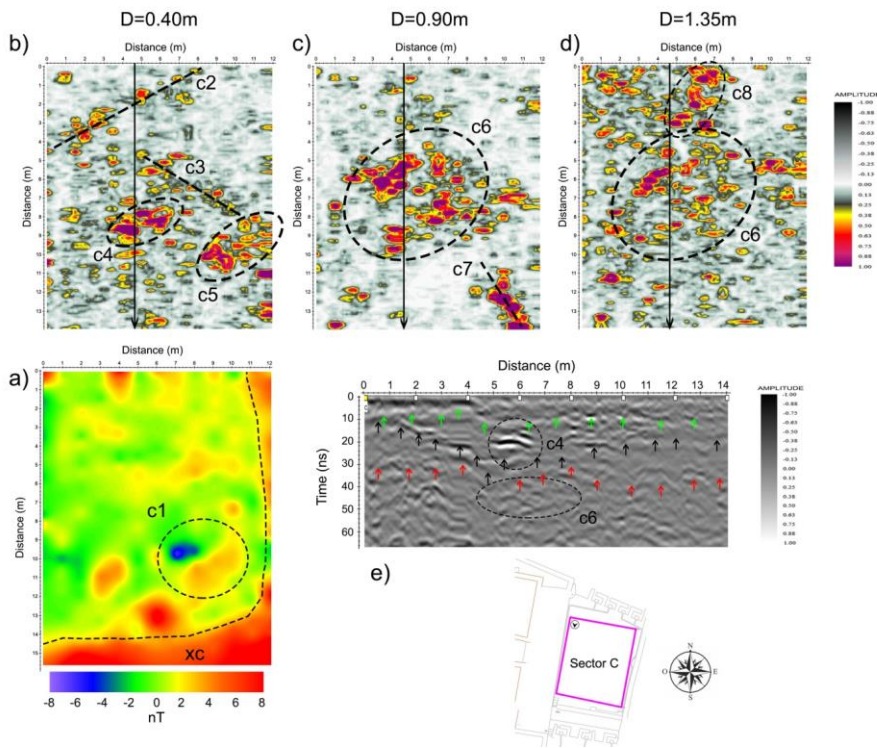
487 MAG map (Fig.5a) shows the absence of any relevant magnetic alignment. The most significant
488 feature is located along the Southern and the Eastern edges of the map and can be likely related to
489 the perimeter walls presence (anomaly xc). Another anomaly is c1 that is located inside the area
490 where the presence of furrows for soil irrigation have been reported. For this reason it cannot be
491 excluded that c1 is generated by “modern” man-made artefact.

492 The GPR depth slice seems to confirm the absence of relevant reflective areas of archaeological
493 interest. At a depth of 0.40 m, possible alignments are detected (c2 and c3 in Fig. 6b). Considering
494 the discontinuity of the observed anomalies and their limited extension in depth, they could be
495 associated to the presence of drainage channel. Anomalies c4, c5, c6 and c8 possibly identify the
496 presence of collapsed structures, stone blocks and/or rocks.

497 More interesting is c7 that could be generated by archaeological remains or by an elongated
498 geological body.

499 The B-scan showed in figure 5f, acquired at the frequency of 600 MHz, identifies the presence of
500 three main stratigraphic units highlighted in green, black and red arrows at different depths that
501 likely correspond to different archaeological phases of the site. The top and the bottom units (green
502 and red arrows) are mainly horizontal. The intermediate one shows a depression in correspondence
503 of c4. The B-scan also shows the amplitude of the reflection associated to the anomaly c4 and the
504 more chaotic and smaller ones related to anomaly c6.

505
506



507
 508 Fig.6 - Sector C: (a) Z gradiometric map; (b-c-d) GPR depth slices (600 MHz frequency) at theoretical
 509 depths of 40, 90 cm and 135 cm respectively; (e) radargram acquired at 200 MHz in correspondence of the
 510 profile indicated with the black arrows in figure 6b-c-d. . Green, black and red arrows indicate the presence
 511 of three anthropogenic layers (with this regard see caption of Fig. 5).

512

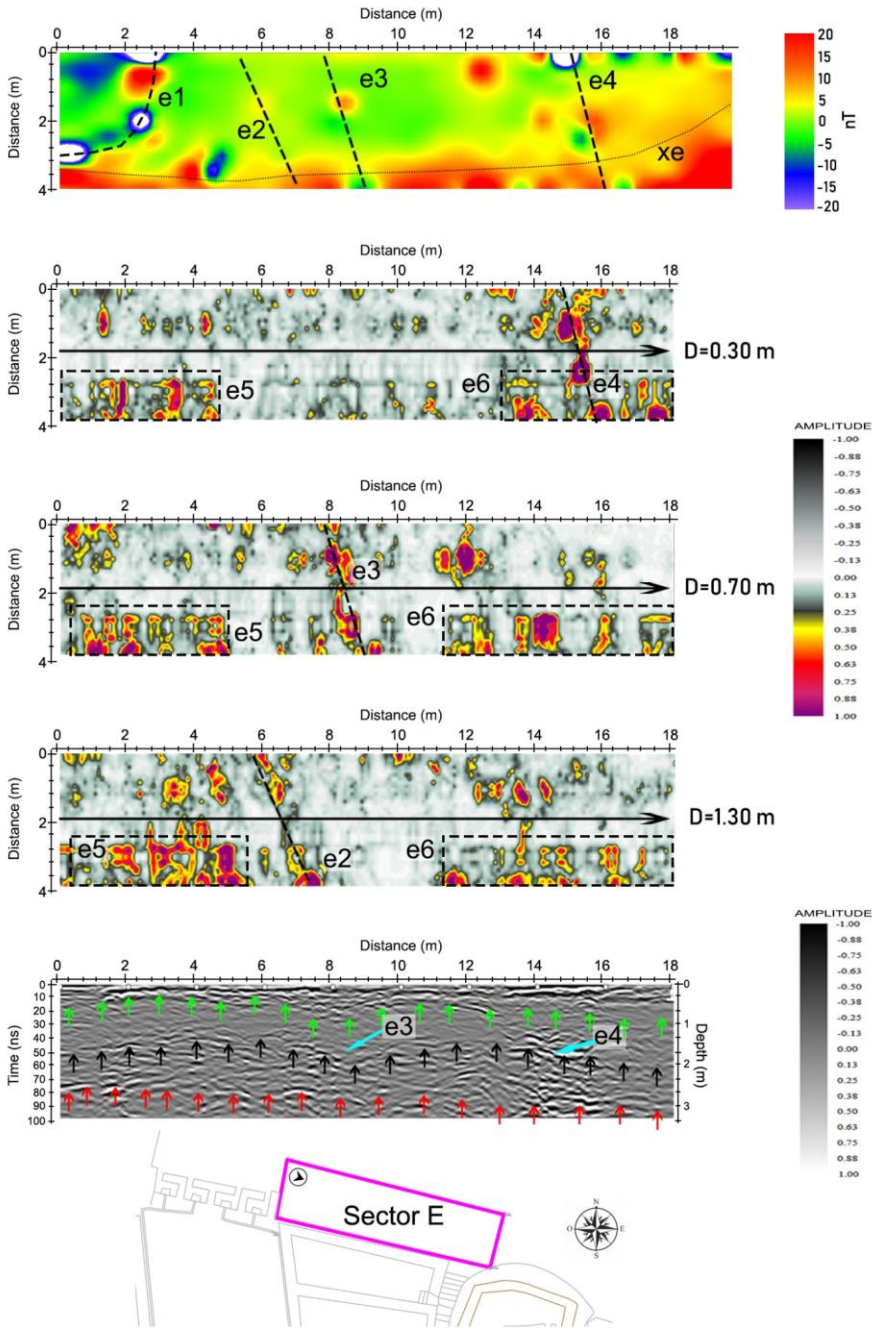
513 4.4 Sector E

514 The magnetometric investigation was carried out according to a grid of 4 x 18 m with longitudinal
 515 acquisitions towards the East and a spacing of 1 meter. In addition, GPR profiles were acquired
 516 only in the longitudinal direction using the same grid of 4x18m as for MAG with a spacing of the
 517 acquisitions every 0.5m and direction towards the East.

518 The lower part of the magnetic map (Fig. 7a) is significantly influenced by the presence of the
 519 confining wall (anomaly xe). Other anomalies are indicated as e1 – 4. Among these, e1 is the only
 520 clearly visible. It is mainly constituted by three dipolar anomalies thus suggesting that is not related
 521 to a continuous body (geological or archaeological). As regard as e2 – 4, they have been traced on
 522 the base of GPR data analysis (Fig. 7b-d) where they are associated to the presence of N-S

523 elongated anomalies, probably related to the presence of shallow remains such as channels. In
524 addition, there are strong reflections in areas e5 and e6. These reflective areas clearly suggest the
525 presence of functional and constructive relationships with the structures of the ceremonial baths of
526 the plaza undida (sector A). In particular, the shapes of e5 and e6 imaged at depths from 30cm to
527 1.30m are very similar to the walls of the ritual baths of the western *plaza undida*. This suggests a
528 different plant of the western plaza undida in the past before the current spatial configuration. As a
529 consequence the building between the current western plaza undida and the central nucleus was
530 added later so modifying the shape of the same plaza undida.

531



533 Figure 7. Sector E. (a) The investigated area; (b) Z gradiometric map; (c-d-e) Georadar maps (600 MHz
534 frequency) at depth of 50-17, 100-125cm, and 150-175cm respectively; (f) radargram acquired at 600 MHz
535 frequency in correspondence of the profile indicated with the black arrow in Fig.7 cde. Green, black and red
536 arrows identify the presence of three layers at different depths that correspond to different archaeological
537 phases of the site as proved by some trial excavations conducted nearby (Ziolkowski 2016; 2017)

538

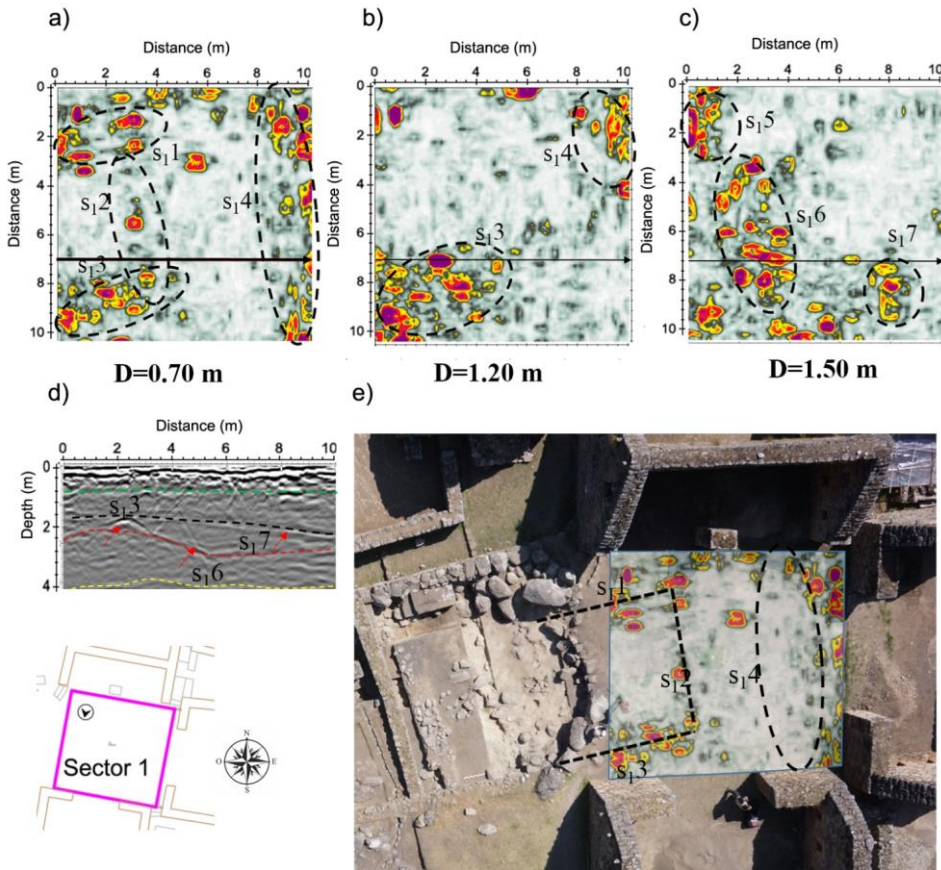
539

540 **4.6 Sector 1**

541 In this sector magnetic survey was not performed due to the presence of rivets stuck in the ground.

542 On the other hand, a GPR investigation was carried out in a 10x10m grid with longitudinal and
543 transverse acquisitions spaced 50 cm and directions, respectively, from west to east and from north
544 to south. 600 MHz depth slices exhibit high values of amplitude, indicated with s_{13} and s_{14} in
545 figure 8a-b-c, at depths between 70 and 120cm referable to stone accumulation to level the square
546 which is more elevated respect to the square of the *huanca*. Being close to the corner of the *kancha*
547 such stone accumulation could be related to collapse material, considering that the area of high
548 radar amplitude increases with depth. At the same time the anomaly s_{13} could be due to a collapsed
549 wall that intercepted two unearthed structures (identified by the anomalies s_{11} and s_{12}) defining a
550 quadrangular area. Similar interpretation could be made for the anomalies s_{16} and s_{17} , found at a
551 depth approximately equal to 1.50 m. These anomalies are oriented of about 15 degrees respect to
552 the sides of the courtyard (Figure 8e). This leads to the hypothesis that these anomalies may refer to
553 a construction phase preceding the courtyard. Such hypothesis is also confirmed by the B-scan
554 showed in figure 8d intercepting the anomalies s_{13} , s_{16} and s_{17} (indicated with red arrows in figure
555 8a). The radargram (figure 8d), acquired at a frequency of 200 MHz, evidences the presence of at
556 least three separated layers associable to three distinct phases. The first one, indicated with green
557 dashed line, should be related to a previous floor, the second and the third, indicated with the red
558 and yellow lines, respectively, refer to two more ancient phases. Some reflectors with hyperbola
559 shape, suggesting the presence of walls or ancient drainage channels, are also visible.

560



561
 562
 563 Figure 8. Sector 1: (a-b-c) GPR depth slices (600 MHz frequency) at depths of about 70, 120, and 150cm,
 564 respectively; (d) radargram acquired at 200 MHz frequency along the profile indicated with the black arrow
 565 in Fig.8 a-b-c-; The green, red and black dashed lines indicated the presence of different archaeological
 566 phases. The red arrows mark the presence of some reflectors with hyperbola shape, suggesting the presence
 567 of walls and drainage channels.
 568
 569
 570 (e) overlapping of the depth slice placed at a depth of 70 cm on the aerial photo of the site characterized by
 571 the recently (and partially) excavated area of sector 3.
 572

573 **4.7 Sector 3: comparing archaeological finds with GPR results**

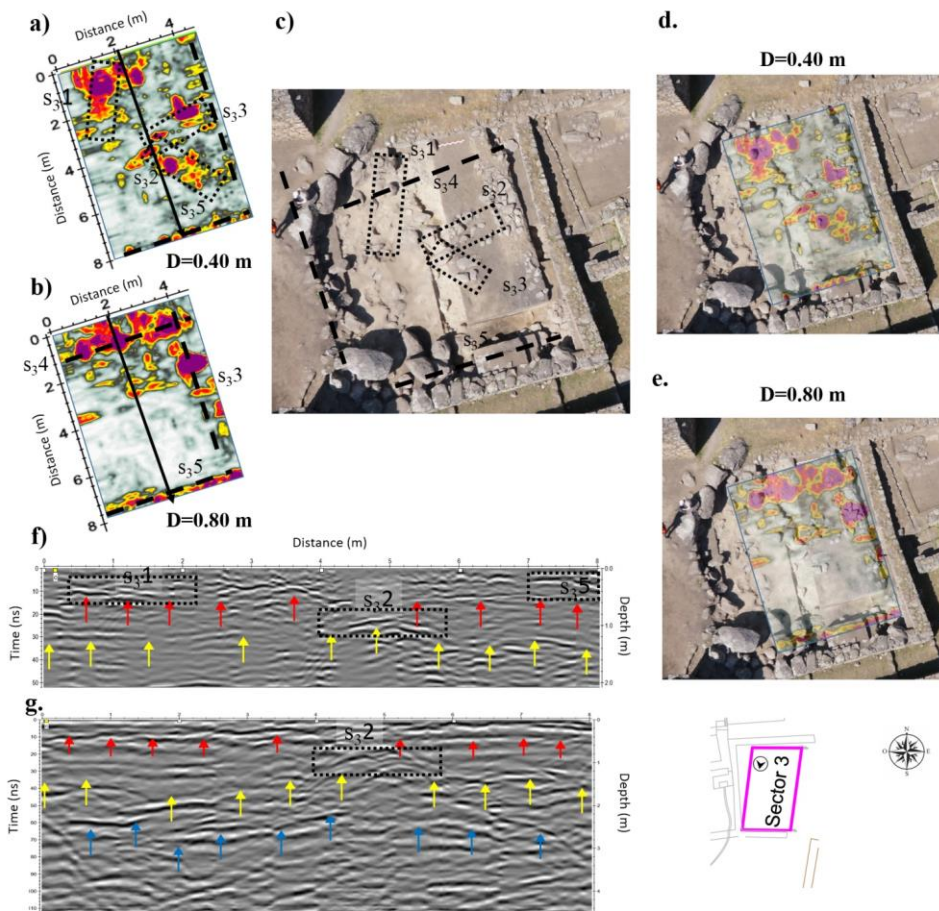
574

575 The georadar survey was performed according to a 5x8m grid with longitudinal and transverse
576 acquisitions and 0.5 meter spacing. After a few months from the geophysical prospections sector 3
577 has been excavated to a depth of approximately 1 m. Therefore, the interpretation of the
578 investigations consists in the comparison between what has been unearthed and what is observed
579 from the geophysical maps.

580 In particular, it can be seen that some stones aligned to form a perpendicular orientation could
581 explain the anomalies s₃₁, s₃₂ and s₃₃ plotted in figure 9(a-b); at the same time, the strong reflective
582 events indicated with s₃₄ and s₃₅ could be associated to the presence of linear structures (walls) of
583 which the second one only partially excavated.

584 The correspondence between the structures brought to light by archaeologists and the reflection of
585 the radar is more evident by observing the radar profiles in Fig. 9f-g where the B-scans at 600 and
586 200 MHz are showed. As in the case of sector 1, also here it is possible observe the presence of
587 three subparallel horizontal reflector due to the presence of different archaeological phases
588 (identified with red, yellow and blue lines in the radargrams), among them it is to be expected that
589 the first two are related to archaeological features while the other one is due to the geological
590 bedrock of the site.

591 The comparative analysis highlights both the potentials and limits of geophysical prospections in
592 detecting structures and artefacts of archaeological interest, especially in less regular contexts and
593 characterized by collapsed walls as in the case of sector 3.



594
595

596 Fig. 9 - Sector 3: (a-b) GPR depth slices (600 MHz frequency) at depths of about 40 and 800cm respectively;
597 (c) aerial photo of the excavated areas with identification of the most interesting GPR anomalies; (d-e) (e)
598 overlapping of the depth slices showed in figure 8a-b on the aerial photo of the investigated area; (f-g)
599 radargrams acquired at 600 and 200 MHz respectively with identification of the main layers associable
600 supposedly to archaeological stratigraphic units (marked by red, yellow and blue arrows).

601
602
603

604 5 Resume and Final remarks.

605 Geophysics as other earth observation technologies only provide indirect data (proxy indicators)
606 related to the presence of archaeological buried remains; therefore, the question is: how is it
607 possible to recognize them? An aid in the interpretation process is given by: (i) the integration of
608

609 results from different geophysical techniques and (ii) the analysis of spatial relationships of the
610 potential archaeological remains, and their spatial and functional relation with emerging
611 architectural evidences. This was the approach adopted in Chachabamba, where the integration of
612 the results from the MAG and GPR survey enabled us to detect a large variety of archaeological
613 features (see figures 9up and 9bottom).

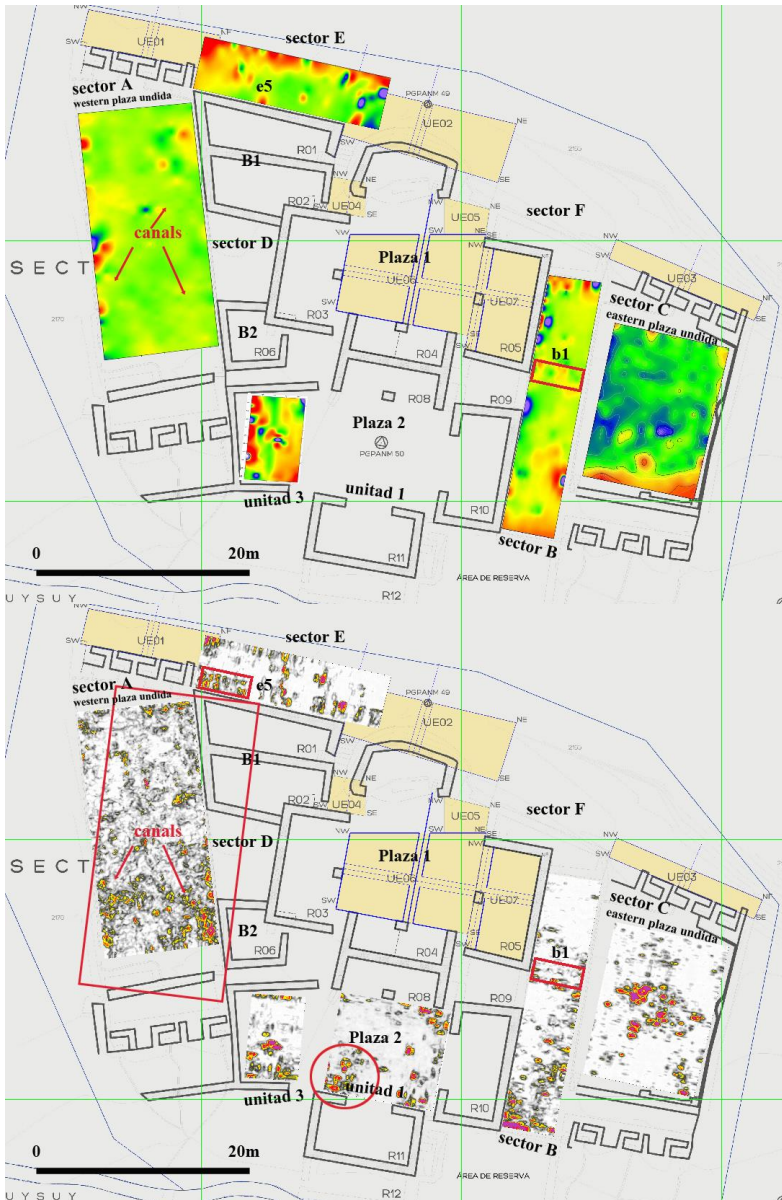
614 The interpretation process of geophysical surveys was possible thanks to the availability of ancillary
615 data related to previous excavations, which facilitated the identification of some archaeological
616 targets such as, walls, canals, morphological changes of terraces, stone blocks and rocks (see in
617 particular sections 4.1 and 4.2). In some cases, the GPR B-scans and time slices allowed the
618 identification of different anthropogenic layers. This confirmed the hypothesis of archaeologists,
619 also supported by trial excavations, according to which the current archaeological area of
620 Chachabamba has not been constructed in a single phase, but, it is the result of at least two or more
621 building phases.

622 Nevertheless, the results so far obtained pose still additional questions, among which that related to
623 the original plan of the *plaza undidas*. In particular, in the western side, the results obtained in
624 sector E put in evidence some reflective (radar) areas characterized by the same shapes as those of
625 the ceremonial baths, still well preserved. (see sector E in Figure 9bottom). Therefore, it is
626 reasonable to argue that, in the past, the western *plaza undida* was different from what it appears
627 today in both shape and dimensions. Moreover, observing the plan, it seems enough clear that the
628 oblique buildings B1 and B2 (in Figure 9bottom) were constructed after the *kancha*, that is the
629 architectural complex around plaza 1 and plaza 2. This suggests that in the original plan the western
630 *plaza undida* was symmetrically laid (as the eastern *plaza undida*), respect to the North-South axis.
631 Subsequently, the western *plaza undida* (see red rectangular block in Figure 9bottom) was moved
632 and rotated to make room to buildings B1 and B2 (see Fig.9bottom).

633 Additionally, the results from the integration of MAG and GPR show anomalies referable to: i)
634 structures (see red circle in Fig.9bottom) preceding plaza 2, ii) some canals in the western *plaza*
635 *undida*; iii) buried walls in continuity with emerging structures (see small red rectangular box in
636 sector B, Fig. 9bottom).

637 In conclusion, the geophysical results we obtained shed new light on the Chachabamba
638 archaeological area, where there are rich buried remains that still wait to be excavated and
639 numerous pieces of its puzzled history to be revealed. Moreover, Chachabamba presents all the
640 typical architectural and functional features that are also present in the ceremonial and
641 administrative sites of Urubamba valley. Therefore, the successful results we obtained in

642 Chachabamba encourage to adopt the same methodological approach for other sites in to the sacred
643 valley which also includes Machu Picchu.
644



645
646
647 Figure 10. (up) magnetic maps; (bottom) georadar maps at depth of 75 cm.
648

Acknowledgments

649

650

651 The research was funded by the National Science Centre of Poland (grant OPUS nr UMO-
652 2015/19/B/HS3/03557). We acknowledge also the support and funding from Italian of CNR and
653 Italian Ministry of Foreign Affairs

654

655 **Author contributions**

656 N. M. conceived and directed archaeo-geophysical investigations, wrote sections 1 and 5,
657 coordinated sections 3 and 4, contributed to section 4 for archaeo-geophysical interpretation; L.C.
658 acquired and processed GPR data and wrote section 3.2.1 and contributed to section 4 with
659 particular reference to GPR results discussion; G.R. acquired and processed MAG data, wrote
660 sections 3.2.2, contributed to section 4 with particular reference to GPR results discussion. M. S.
661 contributed to GPR and MAG data acquisition, wrote section 2.2; D.S. contributed to section 2,
662 with particular reference to state-of-the art of investigations, and the archaeological interpretation in
663 section 4; F.A., J.B., M.Z. contributed to section 2 with particular reference to state-of-the art of
664 investigations, R.L. revised the whole paper, wrote with N.M. section 1, contributed to sections 4
665 and 5.

666

667

668

669 **References**

670

Aitken MJ, Webster G, Rees A (1958) Magnetic Prospecting. *Antiquity*, 32, 270–271.

671

Aspinall A, Gaffney C, Schmidt A (2008) *Magnetometry for Archaeologists. Geophysical methods for
archaeology.* Altamira Press. Lanham, 189-201.

672

Best M, Bobrowsky P, Douma M, Carlotto V, Pari W (2009) Geophysical Surveys At Machu Picchu,
Peru: Results For Landslide Hazard Investigations. In: K. Sassa & P. Canuti (Eds) *Landslides – Disaster
Risk Reduction.* Springer Berlin Heidelberg, pp. 265-273.

673

674

675

Bonomo N, Osella A, Ratto N (2010) Detecting and mapping buried buildings with Ground-Penetrating
Radar at an ancient village in northwestern Argentina. *Journal of Archaeological Science*, 37, 3247-
3255.

676

677

678

Carlotto V, Cardenas J, y Fidel L (2009) La Geología , evolucion geomorfológica y geodinamica
externa de la ciudad Inca de Machupicchu, Cusco-Perù.. *Revista de la Asociación Geológica Argentina*
65(4): 725-747 (2009)

679

680

681

Carlotto V, Cardenas J, y Fidel L (2011) La Geología en la conservación de Machupicchu - Boletín N°1
serie I Patrimonio y Geoturismo. 305pp.

682

Formatted: English (United States)

683 Cuca B, Hadjimitsis DG (2017) Space technology meets policy: An overview of Earth Observation
684 sensors for monitoring of cultural landscapes within policy framework for Cultural Heritage. *Journal of*
685 *Archaeological Science: Reports*, 14: 727–733. DOI: <https://doi.org/10.1016/j.jasrep.2017.05.001>

686 Fejos C (1944) *Archeological Explorations in the Cordillera Vilcabamba Southeastern Peru* – Paul Fejos,
687 New York.

688 Florit CM, Ángel M, Ontiveros C, Goossens L, Meyer C, Sala R, Ortiz H (2018) Geophysical survey of
689 two rural sites in Mallorca (Balearic Islands, Spain): Unveiling Roman villae, *Journal of Applied*
690 *Geophysics*, 150, 2018, 101-117, <https://doi.org/10.1016/j.jappgeo.2017.12.014>.

691 Gavazzi A (2010) *Arquitectura Andina. Formas e historia de los espacios sagrados*. Apu Graph
692 Ediciones/Lima - Jaca Book/Milano - Hazan/Paris.

693 Goodman D and Piro S (2009) Ground penetrating radar (GPR) surveys at Aiali (Grosseto). In: Campana
694 S, Piro S (eds) *Seeing the un-seen. Geophysics and landscape archaeology*. Taylor and Francis, London,
695 pp 297–302. ISBN 978-0-415-44721-8

696 Gumaer DR (1985) *Preliminary Report of Geophysical Surveying at the Nanchoc Cemetery Site*. Ms. on
697 file, Department of Anthropology, University of Kentucky, Lexington

698 Henderson KK (2004). *Ground-penetrating radar at Tiwanaku, Bolivia*. Unpublished MA thesis,
699 Department of Anthropology, University of Denver.

700 Keay SJ, Parcak SH, Strutt KD (2014) High resolution space and ground-based remote sensing and
701 implications for landscape archaeology: the case from Portus, Italy. *Journal of Archaeological Science*,
702 52, 277–292. <http://dx.doi.org/10.1016/j.jas.2014.08.010>.

703 Kvamme KL (2003) Geophysical surveys as landscape archaeology. *American Antiquity*, 68(3): 435–
704 457. doi: 10.2307/3557103

705 Larson DO, Lipo CP, Ambos EL (2003) Application of advanced geophysical methods and engineering
706 principles in an emerging scientific archaeology. *First Break*, 21, 51–62

707 Lasaponara R, Leucci G, Masini N, Persico R, Scardozzi G (2016) Towards an operative use of remote
708 sensing for exploring the past using satellite data: The case study of Hierapolis (Turkey). *Remote*
709 *Sensing of Environment* 174, 148-164

710 Lasaponara R, Masini N, Pecci A, Perciante A, Pozzi Escot D, Rizzo E, Scavone M, Sileo M (2017)
711 Qualitative evaluation of COSMO SkyMed in the detection of earthen archaeological remains: The case
712 of Pachamacac (Peru). *Journal of Cultural Heritage*, <http://dx.doi.org/10.1016/j.culher.2015.12.010>

713 Lasaponara R, Leucci G, Masini N, Persico R (2014) Investigating archaeological looting using satellite
714 images and GEORADAR: the experience in Lambayeque in North Peru. *Journal of Archaeological*
715 *Science*, 42, 216-230, <http://dx.doi.org/10.1016/j.jas.2013.10.032>

Field Code Changed

Field Code Changed

716 Lasaponara R, Masini N (2008) Advances in Remote Sensing for Archaeology and Cultural Heritage
717 Management, Proc. of I International EARSeL Workshop “Advances in Remote Sensing for
718 Archaeology and Cultural Heritage Management”, Rome 30 septembre-4 October, 2008, Aracne,
719 Roma, 2008. ISBN: 978-88-548-2030-2

720 Lascano E, Osella A, de la Vega M, Buscaglia S, Senatore X, Lanata JL (2003) Geophysical prospection
721 at Florida blanca archaeological site, San Julián Bay, Argentina. *Archaeological Prospection*, 10, 175-
722 192.

723 Leucci G, De Giorgi L, Di Giacomo G, Ditaranto I, Miccoli I, Scardozi G (2016) 3D GPR survey for
724 the archaeological characterization of the ancient Messapian necropolis in Lecce, South Italy, *Journal of*
725 *Archaeological Science* 2016, Volume 7, Pages 290-302, <https://doi.org/10.1016/j.jasrep.2016.05.027>.

726 Ludeno G, Capozzoli L, Rizzo E, Soldovieri F, Catapano I (2018). A microwave tomography strategy
727 for underwater imaging via Ground Penetrating Radar, *Remote Sens.* 10(9),
728 1410; <https://doi.org/10.3390/rs10091410>

729 Malfitana D, Leucci G, Fragalà G, Masini N, Scardozi G, Cacciaguerra G, Santagati C, Shehi E (2015)
730 The potential of integrated GPR survey and aerial photographic analysis of historic urban areas: A case
731 study and digital reconstruction of a Late Roman villa in Durrës (Albania). *Journal of Archaeological*
732 *Science* 4. pp. 276-284. ISSN 2352-4103

733 Masini N, Marzo C, Manzari P, Belmonte A, Sabia C, Lasaponara R (2018) On the characterization of
734 temporal and spatial patterns of archaeological crop-marks. *Journal of Cultural Heritage*, doi:
735 [10.1016/j.culher.2017.12.009](https://doi.org/10.1016/j.culher.2017.12.009)

736 Masini N, Rizzo E, Capozzoli L, Leucci G, Pecci A, Romano G, Sileo M, Lasaponara R (2016). Remote
737 Sensing and Geophysics for the Study of the Human Past in the Nasca Drainage. In: Lasaponara R.,
738 Masini N., Orefici G. (Eds). *The Ancient Nasca World New Insights from Science and Archaeology*.
739 Springer International Publishing, 2016, pp. 469-527, doi: [10.1007/978-3-319-47052-8_20](https://doi.org/10.1007/978-3-319-47052-8_20)

740 Masini N, Capozzoli L, Chen P, Chen F, Romano G, Lu P, Tang P, Sileo M, Ge Q, Lasaponara R (2017)
741 Towards an operational use of geophysics for Archaeology in Henan (China): Archaeogeophysical
742 investigations, approach and results in Kaifeng. *Remote Sensing* 2017, 9 (8), 809, doi:
743 [10.3390/rs9080809](https://doi.org/10.3390/rs9080809)

744 Nair S., (2015) *At Home with Sapa Inca: Architecture, Space and Legacy at Chinchero*. Austin (TX):
745 University of Texas Press, ISBN 978-1-4773-0250-7

746 Oviedo M, Concha R, Astete I, Cárdenas J, Flores T, y Carlotto V., 2011 – Geología y geodinámica del
747 camino sagrado en Machupicchu. Boletín N°1 serie I Patrimonio y Geoturismo, 238-244
748 Primers H (2006) Improntas de esteras en cerámica prehispánica del sitio Bella Vista (Depto. Beni, Bolivia) Actas
749 III Jornadas Internacionales sobre Textiles Precolombinos. Departament d'Art de la Universitat

Field Code Changed

Formatted: English (United Kingdom)

750 Autonoma de Barcelona - Institut Catala Iberoamericana, Barcelona, In: Solanilla Demestre, V. (Ed.) pp.
751 207-212

752 Opitz R, Herrmann J (2018) Recent trends and Long-standing Problems in Archaeological Remote
753 Sensing. *Journal of Computer Applications in Archaeology*. 1(1), pp.19–41.
754 DOI: <http://doi.org/10.5334/jcaa.1>

755 Pipan M, Baradello L, Forte E, Finetti I (2001) Ground penetrating radar study of iron age tombs in
756 southeastern Kazakhstan. *Archaeol. Prospect.*, 8, 141–155

757 Piro S, Sambuelli L, Godio A, Taormina R (2007) Beyond image analysis in processing
758 archaeomagnetic geophysical data: case studies of chamber tombs with dromos. *Near Surface*
759 *Geophysics*, 5(6), 405–414.

760 Plachetka UC (2015) The significance of Andean terraces for indigenous knowledge on agro-ecology:
761 The Moray puzzle. Uwe Plachetka, 13pp

762 Qin T, Zhao Y, Lin G, Hu S, An C, Geng D, Rao C (2018) Underwater archaeological investigation
763 using ground penetrating radar: A case analysis of Shanglinhu Yue Kiln sites (China). *Journal of Applied*
764 *Geophysics*, 154, Pages 11-19, <https://doi.org/10.1016/j.jappgeo.2018.04.018>.

765 Radhakrishna Murthy, I. V. (1998) Gravity and Magnetic Interpretation in Exploration, *Geophysics*.
766 *Memoir 40 of the Geological Society of India (Bangalore)*.

767 Rizzo E, Masini N, Lasaponara R, Orefici G (2010) ArchaeoGeophysical methods in the Templo del
768 Escalonado (Cahuachi, Nasca, Perú), *Near Surface Geophysics*, 8 (5), 433-439, doi:10.3997/1873-
769 0604.2010030

770 Sandmeier KJ (2016) ReflexW Version 8.1. Program for Processing of Seismic, Acoustic or
771 Electromagnetic Reflection, Refraction and Transmission Data. Software Manual, Karlsruhe, Germany,
772 628 p.

773 Trinks I, Neubauer W, Hinterleitner A (2014) First high-resolution GPR and magnetic archaeological
774 prospection at the Viking age settlement of Birka in Sweden. *Archaeol. Prospect.* 2014, 21 (3) 185–199.

775 Vanvalkenburgh P, Walker CP, Sturm JO (2015) Gradiometer and Ground-penetrating Radar Survey of
776 Two Reducción Settlements in the Zaña Valley, Peru. *Archaeol. Prospect.*, 22 ,117 – 129. DOI:
777 10.1002/arp.1499

778 Ziolkowski M (2016). Informe anual 2016 - Programa de Investigaciones Arqueológicas e
779 Interdisciplinarias en el Santuario Histórico de Machupicchu, 2016

780 Ziolkowski M (2017). Informe final 2014-2017 - Programa de Investigaciones Arqueológicas e
781 Interdisciplinarias en el Santuario Histórico de Machupicchu

782

Field Code Changed

Field Code Changed

